Detection of Zn2+ ion on a reusable fluorescent mesoporous silica beads in aqueous medium

ARTICLE *in* JOURNAL OF INCLUSION PHENOMENA · DECEMBER 2013

Impact Factor: 1.49 · DOI: 10.1007/s10847-012-0238-1

5 AUTHORS, INCLUDING:

Mohammad Shahid
Indian Institute of Technology Delhi
32 PUBLICATIONS **330** CITATIONS
SEE PROFILE

Arvind Misra
Banaras Hindu University
48 PUBLICATIONS **432** CITATIONS
SEE PROFILE

J Incl Phenom Macrocycl Chem (2013) 77:241–248
DOI 10.1007/s10847-012-0238-1

ORIGINAL ARTICLE

Detection of Zn^{2+} ion on a reusable fluorescent mesoporous silica beads in aqueous medium

Mohammad Shahid · Priyanka Srivastava · Syed S. Razi · Rashid Ali · Arvind Misra

Received: 17 May 2012 / Accepted: 10 August 2012 / Published online: 22 August 2012

Abstract An efficient sensor system was designed and built by immobilizing a fluorescent bischromophoric dyad through a sol–gel reaction on mesoporous silica beads of high surface area. The silica supported dyad, **SSD** containing anthracene and naphthalimide moieties have shown high sensitivity and selectivity to detect Zn^{2+} among the tested cations in aqueous medium. The Job's plot analysis showed a 1:1 stoichiometry for a complexation between **SSD** and Zn^{2+} in which the relative fluorescence intensity enhanced, ~6 times due to restricted photoinduced electron transfer reaction and color of the beads were changed from a fluorescent yellow green to blue. The reversible mode of complexation was tested in the presence of EDTA.

Keywords Dyad · SSD · Zn^{2+}

Introduction

The recognition of anions and cations has received considerable attention because of their important roles in biological and environmental processes [1–3]. In biological system Zn(II) is the second most abundant transition metal ion [4] and the concentration of zinc in human body is variable in different physiological environment [5]. Biologically Zn(II) is essential for multiple metabolic activities such as, neural signal transmission, enzyme regulations and gene transcription [4, 6, 7]. A disorder in zinc metabolism is associated with several neurological diseases such as Alzheimer's and Parkinson's [6, 7]. Among the competitive cations (Ca^{2+}, Mn^{2+}, Fe^{3+}, Co^{2+}, Cu^{2+}, Cd^{2+} and Hg^{2+}) detection of Zn(II) is difficult since the $3d^{10}4s^0$ electronic configuration make it spectroscopically silent toward the conventional optical techniques. The fluorescence spectroscopic technique is one of the most efficient method in diagnostic as it offers high sensitivity and selectivity [4, 6, 7]. In this regard, sensing of Zn^{2+} ion through a coordinate and/or covalent bonding has attracted several research groups to develop efficient fluorescent chemosensors which can demonstrate enhanced fluorescence upon recognizing the specific metal ion.

The typical motifs of such kind of sensory systems include an ion-binding receptor site well connected via a spacer arm to one or more photoresponsive chromophoric units, and generate good optical signals upon interaction with different analytes [8]. Based on this approach some efficient fluorescent sensors utilizing quinoline, picoline and fluorescein derivatives have been developed for the detection of zinc ions [9–13]. However, most of the reported fluorescent chemosensors for zinc suffers from low solubility, increase in autofluorescence, fluorescence quenching, irreversible changes in the biological systems due to UV exposure, and so on [14]. To overcome these problems smart organic or inorganic frameworks containing multiple binding sites and capable to increase the analyte–receptor interaction [15] may be of great use to detect zinc ions in a medium.

Recently, modified surface of alumina, silica and/or their nanostructure materials coupled with suitable fluorophores have been developed to detect biologically important heavy metal ions [16, 17]. The rigidity and porosity of ordered mesoporous silica material have advantages to functionalize these materials with desired organic entity [18, 19]. Silica gel

Electronic supplementary material The online version of this article (doi:10.1007/s10847-012-0238-1) contains supplementary material, which is available to authorized users.

M. Shahid · P. Srivastava · S. S. Razi · R. Ali · A. Misra (✉)
Department of Chemistry, Faculty of Science,
Banaras Hindu University, Varanasi 221 005, India
e-mail: arvindmisra2003@yahoo.com; amisra@bhu.ac.in

is amorphous inorganic material having siloxane groups in the bulk and abundant silanol (Si–OH) functions on the surface that can be frequently modified to attach a suitable fluorescent unit. The high surface area and the availability of silanol functional groups on the surface allow covalent immobilization of the organic moieties in high density which, in turn are helpful to transduce the sensing event to a higher response in optical diagnostic applications and in protection of signaling molecule [20] with optical transparency in the visible region [21]. Further, the silica-based nanoparticles have been employed by several research groups for biomedical and environmental research applications successfully such as, bioseparation, drug targeting, cell isolation, enzyme immobilization, protein purification [22, 23] and sensors for the detection of ATP [24], fluoride [25], and copper [26]. Pal et al. [27] reported a novel fluorescent zinc sensor by immobilizing quinoline derivative on an ordered mesoporous silica material, MCM-41.

The receptor-immobilized silica particles based solid chemosensors have some significant advantages and can be utilized as adsorbent in heterogeneous solid–liquid phases [28]. Additionally, the immobilized receptors on an inorganic support can remove guest molecules (toxic metal ions and anions) from the pollutant solution and the nanomaterials can be easily recycled from pollutants by simple filtration method. Thus, after a suitable chemical treatment and washing steps the solid supported sensor, as a semi-permanent sensor [29–31] can be utilized repeatedly, to detect ions. Motivated from this approach we herein report a sensor design based on fluorescent bis chromophoric dyad containing naphthalimide and anthracene moieties well connected through an aminoalkyl linker arm. The dyad system was immobilized on mesoporous silica of high surface area through a well known sol–gel method for a selective and sensitive detection of Zn^{2+} in aqueous medium. **SSD** has shown high binding affinity for Zn^{2+} selectively, with enhanced emission signal due to restricted photoinduced electron transfer (PET) reaction.

Results and discussion

Synthesis of solid supported dyad (**SSD**)

Scheme 1 depicts a synthetic chemical reaction pathway to obtain mesoporous **SSD** containing naphthalimide and anthracene chromophoric units. 4-Bromo-1,8-naphthalicanhydride and aminopropyltriethoxysilane were taken in anhydrous 1,4-dioxane and stirred the reaction mixture for 5 h at ~60 °C to obtain 4-bromo-*N*-propyltriethoxysilyl-1,8-naphthalimide, **2** (Figs. S1, S2). Compound **2** was subsequently refluxed with ethylenediamine in anhydrous pyridine, containing TEA for 6 h to afford a yellow color semisolid compound **3** (Figs. S3, S4). Compound **3** and 9-chloromethylanthracene were constituted in anhydrous *N,N′*-dimethylformamide (DMF) and stirred the solution in the presence of KI and K_2CO_3 at room temperature to afford a yellow color compound **4** in ~52 % yield. Compound **4** was characterized by FT-IR, NMR and ESI–MS spectral data analysis. The FT-IR spectrum of **4** (Fig. S5) showed N–H stretching vibration band at 3,430 cm^{-1} along with C–H and C=C vibration bands at 2,940 and 1,580 cm^{-1} respectively. The stretching vibration band appeared at 1,113 cm^{-1} may be attributed to Si–O–CH_2– functions. Similarly, ^{1}H NMR spectrum of **4** (Fig. S6) showed a broad singlet at δ 6.3 ppm attributable to aromatic –NH resonance along with multiplet

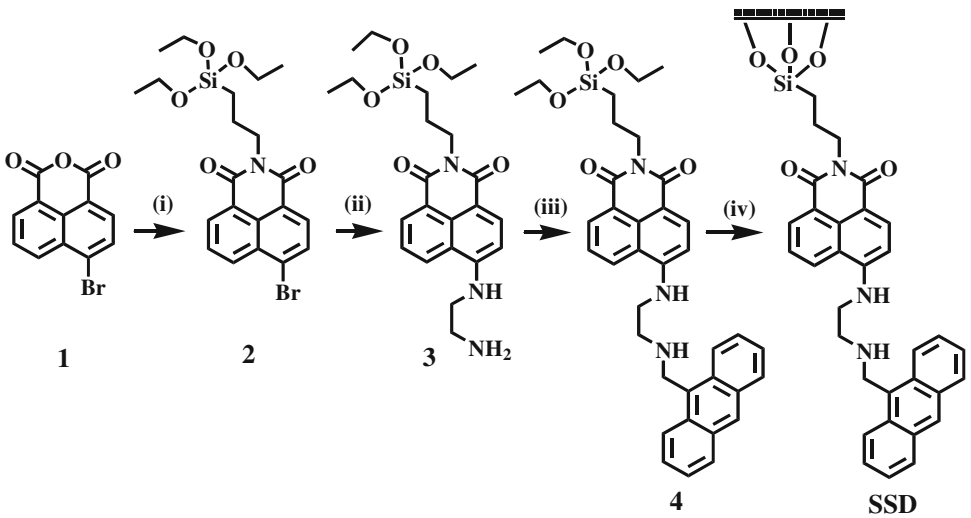

Scheme 1 *i* Aminopropyltriethoxysilane, anhydrous 1,4-dioxane/Δ/5 h, *ii* ethylenediamine, pyridine, TEA/reflux/6 h, *iii* 9-chloromethylanthracene, anhydrous DMF/KI/K_2CO_3/12 h/r.t., *iv* anhydrous DMSO/mesoporous silica/Δ/8 h

of triethoxysilane units at δ 3.85 (for $-CH_2$) and triplet at δ 1.25 ppm ($-CH_3$) respectively. The second –NH proton is overlapped with NCH_2– unit which is resonated at δ 3.42 ppm. The $-CH_2$ attached to Si atom shifted upfield and resonated as triplet at δ 0.659 ppm. The aromatic ring protons were resonated in the range δ 6.60–8.55 ppm. ^{13}C NMR spectrum of **4** showed resonance for Si–CH_2 function at δ 10.93 ppm and a typical resonance attributed to C=O carbon at δ 163.55 ppm (Fig. S7). The resonances attributed to aliphatic region carbon were found at δ 58.1, 47.1, 40.8, 38.6, 22.9, 18.6 ppm while the aromatic carbons resonated in the range δ 104.4–149.5 ppm respectively. A molecular ion $[M+H]^+$ peak appeared at *m*/*z* 650 (calculated *m*/*z* is 649; molecular formula $C_{38}H_{43}N_3O_5Si$) in the ESI–MS spectrum (Fig. S8) confirms the formation of **4.** The peak at m/z 191 is probably due to the formation of a thermodynamically stable 9-anthranylmethyl carbocation by the cleavage of C–N bond between the anthracene and aminoalkyl linker arm [32].

For a successful immobilization of dyad on a mesoporous silica gel, sol–gel method was adopted. The triethoxysilyl functional unit was introduced in the naphthalimide moiety to facilitate immobilization process on the silica gel surface which has itself silanol functionality and both in turn have specificity for each other to develop silyl-etheral (–Si–O–Si–) linkages [33]. The silane compound **4** and silica particles were stirred under anhydrous condition in DMSO for 8 h at 70 °C then stirred further overnight at room temperature. The yellow–green colored particles of **SSD** so fabricated was filtered and washed extensively with methanol and ether. The mesoporous material was dried gently under vacuum at 60 °C and characterized by FT-IR and ^{29}Si NMR spectral data. The FT-IR spectrum (Fig. 1) of **SSD** with respect to free silica gel provided a solid evidence for the attachment of dyad on to the mesoporous silica surface. FT-IR spectrum of **SSD** exhibited bands at 1,087 cm^{-1} attributed to –Si–O–Si– stretching vibration. A broad stretching vibration band around 3,388 cm^{-1} and bands at 1674, 1654 cm^{-1} may be assigned to N–H and C=O functional groups of **SSD**, respectively. The C–H and C=C stretching bands for aliphatic and aromatic vibrations were appeared at 2933, 3058 and 1587 cm^{-1} respectively. Further, ^{29}Si NMR spectrum (Fig. S9) showed resonances at $\delta -39.39$ and -59.99 ppm, probably attributable to terminal and cross-linked siloxane groups, while a broad resonance appeared at $\delta -107.2$ ppm may be assigned to the bulk silica [27] thus, suggested the presence of Si–C bond on the modified surface of **SSD**.

Optical behavior of SSD and metal ion interaction studies

The absorption spectrum of **SSD** in PBS buffer (0.1 M, ACN/H_2O; 1:1, v/v; pH 7.4) illustrated distinctive intramolecular charge transfer (ICT) band ($n \rightarrow \pi^*$) at 440 nm and high energy, $\pi \rightarrow \pi^*$ electronic transition band attributed to anthracene unit, at 368 and 378 nm (Fig. 2). Thus, suggesting the involvement of both the chromophoric units in the optical properties of **SSD**. Similarly, the emission spectra of **SSD** upon excitation at dual wavelengths 378 nm (corresponding to anthracene) or 440 nm (attributed to naphthalimide) displayed a weak emission band at 525 nm. This may be attributed to fluorescence resonance energy transfer or ICT processes [34].

The affinity of **SSD** toward different metal ions was studied in PBS buffer by UV–Vis and fluorescence spectroscopy. Upon addition of different cations such as, Na^+, K^+, Mg^{2+}, Cu^{2+}, Ca^{2+}, Cd^{2+}, Co^{2+}, Ni^{2+}, Ag^+, Hg^{2+},

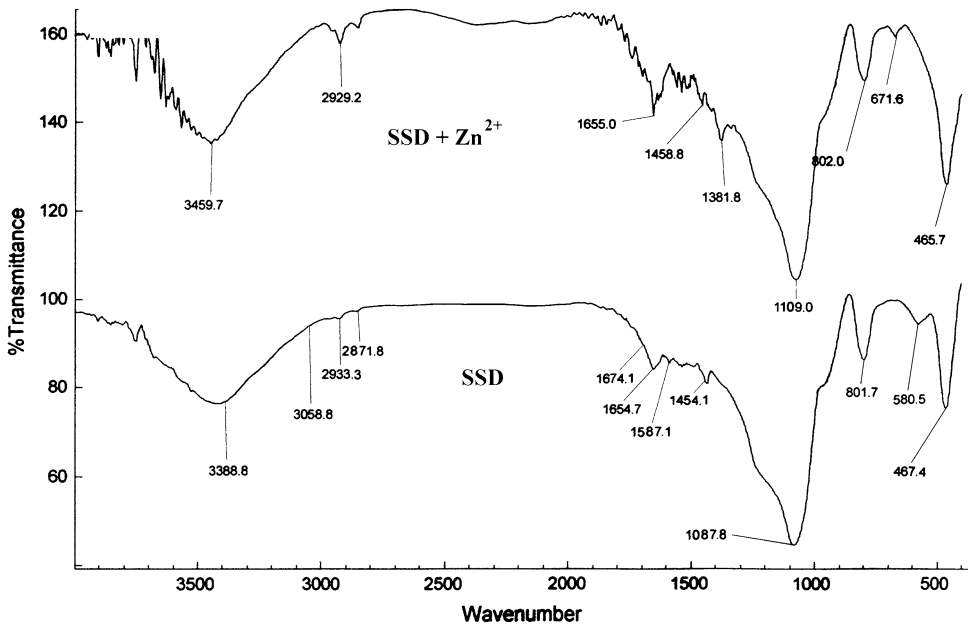

Fig. 1 Stack FT-IR spectra of **SSD** and **SSD** + Zn^{2+} complex

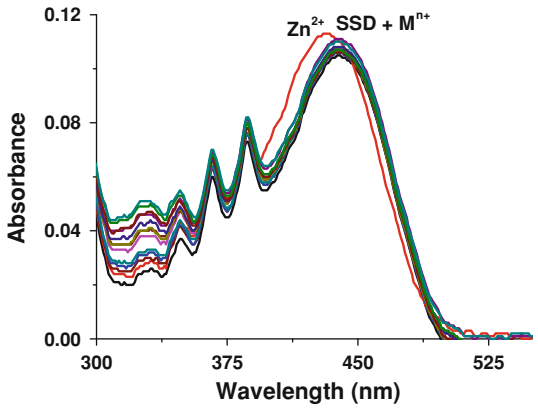

Fig. 2 UV–Vis absorption interaction spectra of **SSD** with different metal ions (100 μM) in PBS Buffer (0.1 M, pH 7.4)

Fe^{3+}, Zn^{2+} (100 μM) to a solution of **SSD** the ICT band centered at 440 nm showed a blue shift, ~15 nm only with Zn^{2+} while insignificant changes were observed with other tested metal ions (Fig. 2). Similarly, the emission spectrum of **SSD** at 378 nm excitation, upon interaction with tested cations exhibited enhanced emission only with Zn^{2+} in which the relative fluorescence intensity centered at ~525 nm amplified ~6 times (turn-On) with a blue shift of ~13 nm. The color of the solution was changed from a weakly fluorescent to highly fluorescent bluish green (switched-On) (inset, Fig. 5) whereas, the color of **SSD** beads in solid state changed from green to highly fluorescent cyano-green under UV light (Fig. 3). The observed chelation enhanced fluorescence may be attributed to coordination of Zn^{2+} through the lone pair electrons available at the nitrogen atom of –NH fragment of aminoalkyl bridging arm connecting both chromophoric units. Thus, the ultimate decreased charge density on the **SSD** restrict the PET reaction to exhibit enhanced fluorescence with a blue shift, consequently. To check the practical ability of **SSD** as a Zn^{2+} selective "turn–On" fluorescent sensor competitive metal ion interaction experiments were performed in which the excess of tested cations (100 μM) were added to a solution of **SSD** containing Zn^{2+} (50 μM) and reversibly by the addition of Zn^{2+} to a solution of **SSD** containing different tested cations. The insignificant change in the emission intensity signal of a complex of **SSD** + $\mathbf{Zn^{2+}}$ suggested high sensitivity and selectivity of **SSD** for Zn^{2+} in the medium (Figs. 4, S10).

To have an idea about binding affinity of **SSD** with Zn^{2+} fluorescence titration experiment was performed. Upon a sequential addition of Zn^{2+} ions (5, 10, 15, 25, 35 and 50 μM) to a solution of **SSD** fluorescence intensity at 525 nm increased gradually (~6 times) along with a blue shift of ~13 nm to appear at 512 nm (Fig. 5). Therefore, suggesting about the complexation of Zn^{2+} with bis-amino function present at the linker arm of **SSD**. The increase in the ground state emission corresponding to both the chromophoric units was obviously attributed to restricted photoinduced electron transfer reaction (Scheme 2). The Job's plot analysis revealed a 1:1 stoichiometry for a complexation between **SSD** and Zn^{2+}. An apparent binding constant estimated by Benesi–Hildebrand method utilizing nonlinear fitting of fluorescence titration data was found to be $K_{assoc} = 1.23 \times 10^5\ M^{-1}$ (inset of Fig. 5). Therefore, indicating relatively high affinity of complexation between **SSD** and Zn^{2+} with a detection limit of 70 nM [35, 36].

Furthermore, among the various sensing system complexation is supposed to be weaker and the reversibility, which is one of the most desired criteria of a good sensing chemistry can be understood by the addition of a strong external additive or a chelating reagent. To ensure the reversible mode of complexation ethylenediaminetetracaetate (EDTA) as a strong chelating reagent was added in excess (200 μM) to a solution of complex, **SSD** + Zn^{2+}. The observed enhanced emission intensity signal due to complexation, **SSD** + Zn^{2+} was decreased almost completely because of relatively high association constant for a complex of EDTA and Zn^{2+} [37]. Reversely, when Zn^{2+} ions were added to a solution of **SSD** containing an excess amount of EDTA insignificant change in relative fluorescence intensity was observed (Fig. 6). This cycle was repeated three times with same final outcome. Thus, the observed emission behavior of **SSD** in the presence of

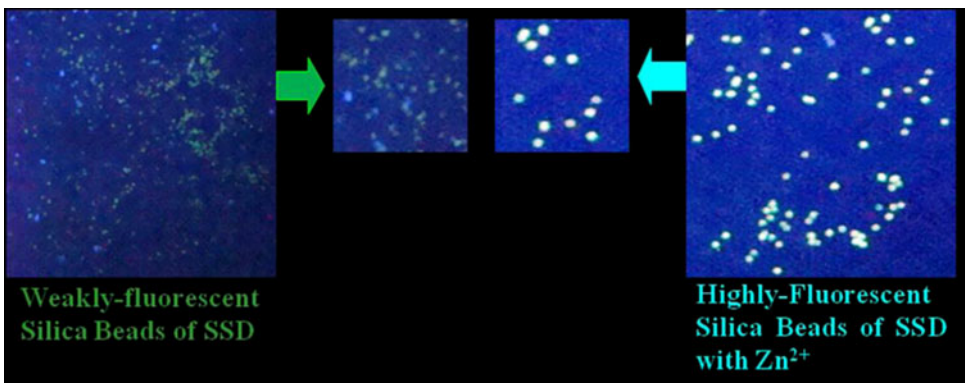

Fig. 3 Image shows the change in color of **SSD** upon interaction with Zn^{2+} ions

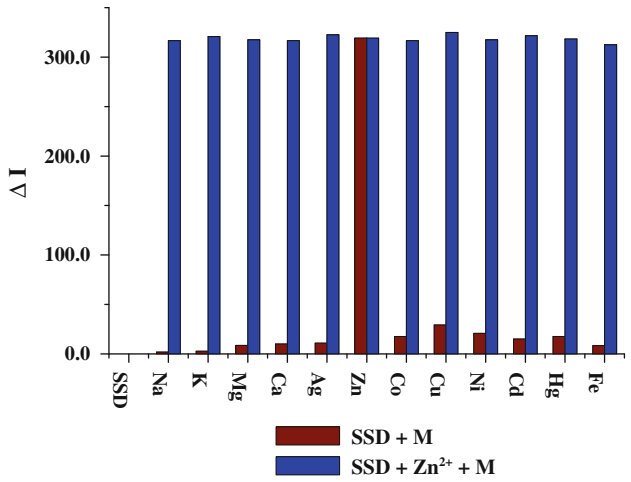

Fig. 4 Metal ions interaction and interference studies of **SSD** with different metal ions in PBS buffer (0.1 M, pH 7.4)

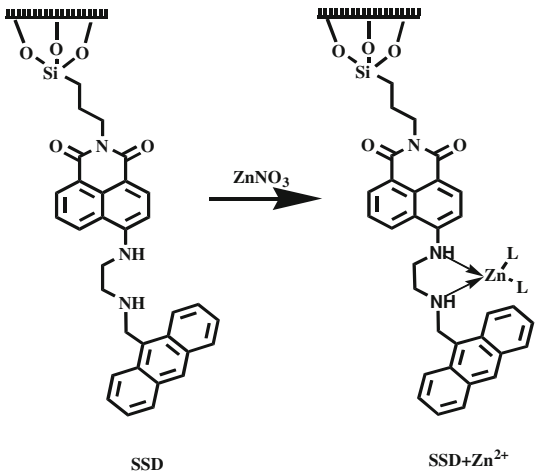

Scheme 2 Plausible mode of complexation of **SSD** with Zn^{2+}

EDTA clearly suggested reversible mode of complexation and adequate selectivity for Zn^{2+} ion. Moreover, FT-IR spectra of **SSD** upon interaction with Zn^{2+} ion, displayed a shift in the N–H stretching vibration band toward higher wave number region, and appeared at 3,448 cm^{-1} along with generation of a new band at 1,381 cm^{-1}. Thus, clearly support the mode of complexation between **SSD** and Zn^{2+} ion through the potential donor sites available in the form of nitrogen atoms of the linker arm (Scheme 2).

Moreover, the pH–emission spectra of **SSD** in the pH range 1–6 exhibited fluorescence enhancement at ~525 nm probably due to the protonation of –NH fragment. However, in the pH range 6.5–14 the relative fluorescence intensity was decreased abruptly between pH 6 and 7.5 and remained constant up to pH 12. Thus, the optical behavior exhibited by **SSD** at different pH may be attributed to a sensitization of naphthalimide unit due to the restricted and enhanced PET process respectively, in which the 4-amino and secondary amine functions present at the bridging linker arm get protonated and deprotonated under acid and alkaline conditions (Fig. 7). The –NH function attached to naphthalimide ring (4-amino) is relatively more acidic than the secondary amine present at the bridging arm. Therefore, 4-amino function attached to naphthalimide unit readily protonated first, in the pH range 1–6 to exhibit enhanced naphthalimide emission. Conversely, in pH range 6.5–7 the same amino function starts deprotonation. That causes a decrease in relative fluorescence intensity of naphthalimide chromophore due to charge propagation. Moreover, in the pH range 7–12 both amino function probably get deprotonated to exhibit combined fluorescence quenching. Thus, in pH range 6.5–8.0 dyad will exhibit diminished fluorescence (turn-Off state) attributed to more charge propagation toward naphthalimide unit. Moreover, it is expected that upon addition of Zn^{2+} ions, as their nitrate salt complexation will be facilitated and consequently,

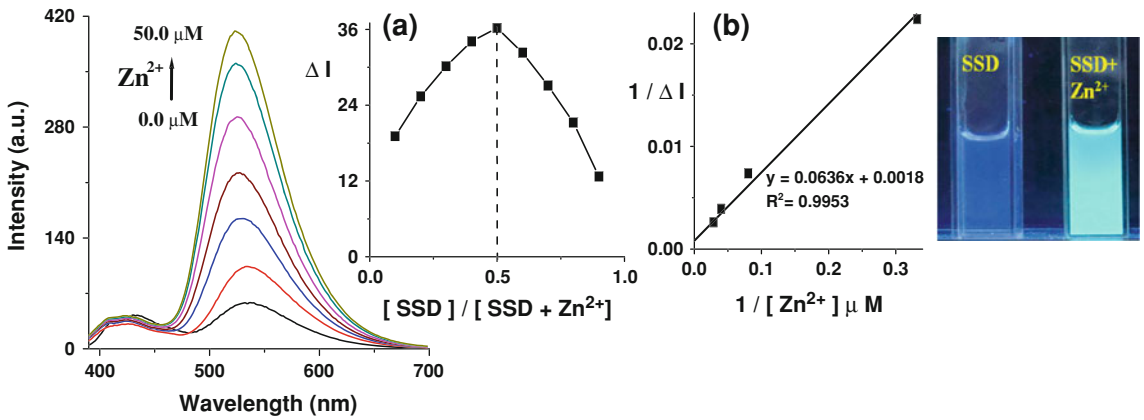

Fig. 5 Fluorescence titration spectra of **SSD** upon interaction with different concentration of Zn^{2+} (0–50 μM) upon excitation at 378 nm in PBS buffer (0.1 M, pH 7.4). *Inset* **a** Job's plot, **b** Benesi–Hildebrand graph and color change of **SSD** upon interaction with Zn^{2+}

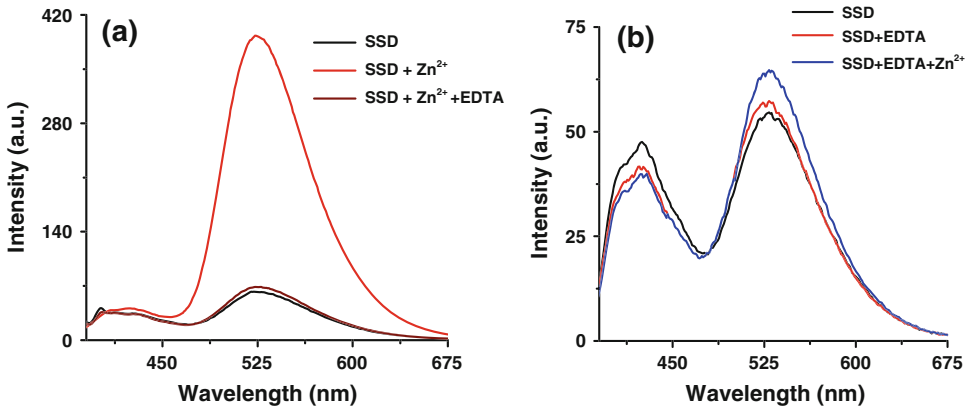

Fig. 6 Change in emission spectra of **SSD a** upon addition of Zn^{2+} (50 μM) then EDTA (200 μM) and **b** upon addition of Zn^{2+} to the solution of **SSD** + EDTA upon excitation at 378 nm

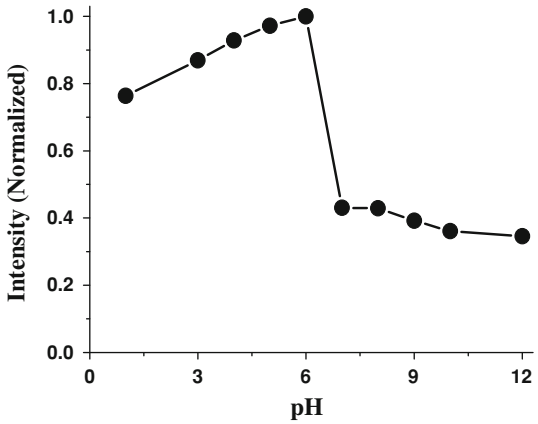

Fig. 7 Fluorescence emission response of **SSD** at different pH at 525 nm

fluorescence enhancement (turn-On) attributed to restricted PET reaction would observe.

Experimental

The absorption and emission spectra were recorded at room temperature on a Shimadzu 1700 spectrophotometer using a quartz cuvette (path length = 1 cm) and CARY Eclipse (VARIAN) fluorescence spectrophotometer at 500 V PMT keeping constant band width of 5 nm/5 nm for emission spectra respectively. FT–IR spectra (KBr pellets) were recorded on a Varian-3100 spectrometer. NMR spectra (chemical shifts in δ ppm) were recorded in $CDCl_3$ on a JEOL AL 300 FT-NMR (300 MHz) spectrometer, using tetramethylsilane as internal standard. Elemental analysis was carried out on CE-440 CHN Analyzer (Exeter Analytical Inc.).

Phosphate buffer (0.1 M) containing sodium chloride was prepared by dissolving Na_2HPO_4 (0.144 g), KH_2PO_4 (0.024 g), NaCl (0.8 g) and KCl (0.02 g) in double distilled water. The pH study [38] was performed by subjecting **SSD** first to pH 1 in PBS buffer. The calculated amount of 1 N NaOH solution was added stepwise to a solution of **SSD** to attain a particular pH and emission spectra were acquired. To establish reversible mode of complexation experiment was carried out by the addition of a chelating reagent, EDTA (200 μM) to a solution of **SSD** containing excess of tested cations and reversibly by the addition of EDTA to a complex solution of **SSD** + Zn^{2+}. To understand stoichiometry in complexation Job's experiment was performed by continuous variation method.

Synthesis of SSD

*Synthesis of 4-bromo-N-propyltriethoxysilyl-1,8-naphthalimide (**2**)*

To a solution of 4-bromo-1,8-naphthalic anhydride, **1** (0.83 g, 3 mmol) in anhydrous 1,4-dioxane (10 ml) aminopropyltriethoxysilane (0.75 ml, 3.5 mmol) was added and stirred the reaction mixture at 60 °C for 5 h under nitrogen atmosphere. After complete reaction (monitored on TLC), the solvent was evaporated under reduced pressure to get off-white color semi-solid compound in ~81 % yield. IR (KBr) υ_{max} (cm^{-1}) 3090 (aromatic C–H str.), 2925 (aliphatic C–H str.), 1650 (C=O str.), 1589, 1386, 1121 (Si–OCH_2–), 1038, 693; ^{1}H NMR (300 MHz, $CDCl_3$) δ (ppm): 8.69 (d, 1H, J = 7.5 Hz, Naphth), 8.59 (d, 1H, J = 8.4 Hz, Naphth), 8.44 (d, 1H, J = 7.8 Hz, Naphth), 8.06 (d, 1H, J = 7.8 Hz, Naphth), 7.87 (*t*, 1H, J_1 = 8.1 Hz, J_2 = 7.8 Hz, Naphth), 3.85 (m, 6H, –OCH_2), 3.50 (*t*, 2H, J_2 = 6.9, 7.2 Hz, –NCH_2), 1.60 (m, 2H, –CH_2), 1.25 (m, 9H, –CH_3), 0.66 (m, 2H, Si–CH_2); Anal. Calc. For $C_{21}H_{26}NO_5BrSi$: C 52.50, H 5.45, N 2.92 %. Found: C 52.81, H 5.76, N, 2.81 %.

*Synthesis of 4-(2-aminoethyl)amino-N-propyltriethoxysilane-1,8-naphthalimide (**3**)*

A solution of compound **2** (0.2 g) as such was taken in anhydrous pyridine (4 ml) and ethylenediamine (3.6 ml,

60.0 mmol) and triethylamine (100 µl) were added. The reaction mixture was refluxed for 6 h under nitrogen atmosphere. After complete chemical reaction solvent was evaporated under reduced pressure and dichloromethane (5 ml) was added. The solvent was evaporated in vacuum to get orange colored semi-solid compound **3** in 54 % yield. IR (KBr) υ_{max} (cm^{-1}): 3400 (N–H str.), 2937 (aliphatic C–H str.), 1653 (C=O str.), 1637, 1573, 1491, 1393, 1286, 1125, 775, 697, 584; ^{1}H NMR (300 MHz, $CDCl_3$) δ (ppm): 8.61 (d, 1H, $J = 7.2$ Hz, Naphth), 8.49 (d, 1H, $J = 8.4$ Hz, Naphth), 8.19 (d, 1H, $J = 8.4$ Hz, Naphth), 7.66 (*t*, 1H, $J_1 = 7.8$ Hz, $J_2 = 7.8$ Hz, Naphth), 6.73 (d, 1H, $J = 8.4$ Hz, Naphth), 6.16 (s, 1H, –NH), 3.85 (m, 6H, $–OCH_2$), 3.41 (m, 4H, $–NCH_2$), 3.20 (m, 2H, $–NCH_2$), 1.57 (m, 2H, $–CH_2$), 1.24 (m, 9H, $–CH_3$), 0.62 (m, 2H, $Si–CH_2$); Anal. Calc. For $C_{23}H_{33}N_3O_5Si$: C 60.10, H 7.24, N 9.14 %. Found: C 61.01, H 7.34, N 9.02 %.

*Synthesis of 4-(2-aminoethyl-N-methenylanthranyl)-N-propyl triethoxysilane-1,8-naphthalimide (**4**)*

To the solution of **3** (0.100 g) in anhydrous DMF (4 ml), 9-chloromethyl anthracene (0.22 g 1.0 mmol) and K_2CO_3 (0.14 g, 1.0 mmol) were taken. A solution of KI (0.17 g, 1.0 mmol in 1 ml DMF) was added dropwise over 1 h to a well stirred reaction mixture. After complete addition reaction mixture was stirred at room temperature for 12 h under nitrogen atmosphere. After complete chemical reaction, the solvent was removed under vacuum and dry DCM was added. Solvent was evaporated to afford compound **4** as a yellow color solid gummy mass. IR (KBr) υ_{max} (cm^{-1}): 3430, 2940, 1656, 1635, 1580, 1357, 1113, 776; ^{1}H NMR (300 MHz, $CDCl_3$) δ (ppm): 8.55 (d, 1H, $J = 7.2$ Hz, Naphth), 8.43 (m, 2H, 1 Naphth + 1 anthracene), 8.38 (m, 2H, 2 anthracene), 8.04 (d, 2H, $J = 3.6, 6.6$ Hz, anthracene), 7.72 (d, 1H, $J = 8.4$ Hz, Naphth), 7.54 (m, 5H, 1 Naphth + 4 anthracene), 6.63 (d, 1H, $J = 8.4$ Hz, Naphth), 6.31 (s, 1H, –NH), 4.86 (s, 2H, $–CH_2$ anthracene), 3.85 (*t*, 6H, $J = 6.9$ Hz, $–OCH_2$), 3.42 (m, 5H, $–NCH_2$ + 1 NH), 3.30 (m, 2H, $–NCH_2$), 1.57 (m, 2H, $–CH_2$), 1.24 (*t*, 9H, $J = 6.9$, 6.6 Hz, $–CH_3$), 0.65 (*t*, 2H, $J = 7.2$, 8.4 Hz, $Si–CH_2$); ^{13}C NMR (75 MHz, $CDCl_3$) δ (ppm): 163.5, 163.2, 136.9, 133.3, 132.1, 131.3, 131.0, 128.4, 127.5, 127.2, 126.6, 126.0, 125.2, 124.0, 122.9, 122.0, 104.4, 58.1, 47.1, 43.6, 40.8, 38.6, 22.9, 18.6, 10.9; Anal. Calc. For $C_{38}H_{43}N_3O_5Si$: C 70.23, H 6.67, N 6.47 %. Found: C 71.15, H 6.71, N 6.34 %; ESI–MS $[M+H]^+$ = found *m/z* 650, calculated *m/z* 649.

Covalent attachment of compound **4** on mesoporous silica beads

The silane compound **4** (g, 0.15 mmol) was dissolved in DMSO (2 ml) and mesoporous silica (0.20 g) was added. The reaction mixture was stirred on a thermomixer at 70 °C for 8 h then further stirred overnight at room temperature. After complete reaction, beads were filtered and washed with methanol and ether. The mesoporous material, yellow–green colored particles of **SSD** was dried gently under vacuum at 60 °C. The **SSD** was characterized by FT-IR and ^{29}Si NMR spectral data. IR (KBr) υ_{max} (cm^{-1}): 3388 (N–H str.), 3058 (C–H aromatic str.), 2933 (C–H aliphatis str.), 1674, 1654 (C=O str.), 1587, 1454, 1087 (Si–O–Si vib), 801, 580, 467. ^{29}Si NMR: δ (ppm): −39.39, −59.99, −107.20.

Complexation of SSD with Zn^{2+}

To a suspension of **SSD** (0.05 g) in acetone (5 ml), $Zn(NO_3)_2$ (0.05 g) was added and mixture was stirred at room temperature for 2 h then filtered and dried to obtain a complex of **SSD**–Zn^{2+}. FT-IR (KBr) υ_{max} (cm^{-1}): 3449 (N–H stretching), 2929 (C–H aliphatic stretching), 1655 (C=O stretching), 1451, 1381, 1109 (Si–O–Si vibration), 802, 671, 465.

Conclusion

In summary, we have demonstrated an efficient method to immobilize fluorescent dyad covalently on mesoporous silica beads, **SSD**. The **SSD** upon interaction with various metal ions exhibited fluorescence enhancement selectively with Zn^{2+} ions. The emission intensity of a complex, **SSD** + Zn^{2+} decrease in the presence of EDTA thus, makes the system reusable and can be utilized repeatedly in the sensing events.

Acknowledgments Authors are thankful to the Council of Scientific and Industrial Research (CSIR), New Delhi for financial support and fellowships (to MS, PS and SSR) and UGC (to RA).

References

1. de Silva, A.P., Gunaratne, H.Q.N., Gunnlaugsson, T., Huxley, A.J.M., McCoy, C.P., Rademacher, J.D., Rice, T.E.: Signaling recognition events with fluorescent sensors and switches. Chem. Rev. **97**, 1515–1566 (1997)
2. Kimura, E., Koike, T.: Recent development of zinc-fluorophores. Chem. Soc. Rev. **27**, 179–184 (1998)
3. Lippard, S.J.: Small-molecule fluorescent sensors for investigating zinc metalloneurochemistry. Acc. Chem. Res. **42**, 193–203 (2009)
4. Jiang, P., Guo, Z.: Fluorescence-based sensing of divalent zinc in biological systems. Coord. Chem. Rev. **248**, 205–229 (2004)
5. Chen, Y., Han, K.-Y., Liu, Y.: Effective switch-on fluorescence sensing of zinc(II) ion by 8-aminoquinolino-β-cyclodextrin/adamantaneacetic acid system in water. Bioorg. Med. Chem. **15**, 4537–4542 (2007)

6. Nolan, E.M., Burdette, S.C., Harvey, J.H., Hilderbrand, S.A., Lippard, S.J.: ZP8, a neuronal zinc sensor with improved dynamic range; imaging zinc in hippocampal slices with two-photon microscopy. Inorg. Chem. **43**, 2624–2635 (2004)
7. Burdette, S.C., Walkup, G.K., Spingler, B., Tsien, R.Y., Lippard, S.J.: Fluorescent sensors for Zn^{2+} based on a fluorescein platform: synthesis, properties and intracellular distribution. J. Am. Chem. Soc. **123**, 7831–7841 (2001)
8. Bergonzi, R., Fabbrizzi, L., Licchelli, M., Mangano, C.: Molecular switches of fluorescence operating through metal centered redox couples. Coord. Chem. Rev. **170**, 31–47 (1998)
9. Zalewski, P.D., Forbes, I.J., Betts, W.H.: Correlation of apoptosis with change in intracellular labile Zn(II) using zinquin [(2-methyl-8-p-toluenesulphonamido-6-quinolyloxy)acetic acid], a new specific fluorescent probe for Zn(II). Biochem. J. **296**, 403–408 (1993)
10. Mikata, Y., Kawata, K., Iwatsuki, S., Konno, H.: Zinc-specific fluorescent response of tris(isoquinolylmethyl)amines (isoTQAs). Inorg. Chem. **51**, 1859–1865 (2012)
11. Majzoub, A.E., Cadiou, C., Dechamps-Olivier, I., Tinant, B., Chuburu, F.: Cyclam-methylbenzimidazole: a selective OFF-ON fluorescent sensor for zinc. Inorg. Chem. **50**, 4029–4038 (2011)
12. Ambrosi, G., Formica, M., Fusi, V., Giorgi, L., Macedi, E., Micheloni, M., Paoli, P., Pontellini, R., Rossi, P.: Efficient fluorescent sensors based on 2,5-diphenyl[1,3,4]oxadiazole: a case of specific response to Zn(II) at physiological pH. Inorg. Chem. **49**, 9940–9948 (2010)
13. Bazzicalupi, C., Bencini, A., Matera, I., Puccioni, S., Valtancoli, B.: Selective binding and fluorescence sensing of Zn^{II} with acridine-based macrocycles. Inorg. Chim. Acta **381**, 162–169 (2012)
14. Liu, Y., Zhang, N., Chen, Y., Wang, L.H.: Fluorescence sensing and binding behavior of aminobenzenesulfonamidoquinolino-β-cyclodextrin to Zn^{2+}. Org. Lett. **9**, 315–318 (2007)
15. Descalzo, A.B., Rurack, K., Weisshoff, H., Martinez-Manez, R., Marcos, M.D., Amoros, P., Hoffmann, K., Soto, J.: Rational design of a chromo- and fluorogenic hybrid chemosensor material for the detection of long-chain carboxylates. J. Am. Chem. Soc. **127**, 184–200 (2005)
16. Balaji, T., El-Safty, S.A., Matsunaga, H., Hanaoka, T., Mizukami, F.: Optical sensors based on nanostructured cage materials for the detection of toxic metal ions. Angew. Chem. Int. Ed. **45**, 7202–7208 (2006)
17. Lee, S.J., Lee, S.S., Lee, J.Y., Jung, J.H.: A functionalized inorganic nanotube for the selective detection of copper(II) ion. Chem. Mater. **18**, 4713–4715 (2006)
18. Mercier, T., Pinnavaia, T.J.: Access in mesoporous materials: advantages of a uniform pore structure in the design of a heavy metal adsorbent for environmental remediation. Adv. Mater. **9**, 500–503 (1997)
19. Koyano, K.A., Tatsumi, T., Tanaka, Y., Nakata, S.: Stabilization of mesoporous molecular sieves by trimethylsilylation. J. Phys. Chem. B **101**, 9436–9440 (1997)
20. Ros-Lis, J.V., Garcia, B., Jimenez, D., Martinez-Manez, R., Sancenon, F., Soto, J., Gonzalvo, F., Valldecabres, M.C.: Squaraines as fluoro-chromogenic probes for thiol-containing compounds and their application to the detection of biorelevant thiols. J. Am. Chem. Soc. **126**, 4064–4065 (2004)
21. Schulz-Ekloff, G., Wohrle, D., van Duffel, B., Schoonheydt, R.A.: Chromophores in porous silicas and minerals: preparation and optical properties. Microporous Mesoporous Mater. **51**, 91–138 (2002)
22. Yi, D.K., Selvan, S.T., Lee, S.S., Papaefthymiou, G.C., Kundaliya, D., Ying, J.Y.: Silica-coated nanocomposites of magnetic nanoparticles and quantum dots. J. Am. Chem. Soc. **127**, 4990–4991 (2005)
23. Abou-Hassan, A., Bazzi, R., Cabuil, V.: Multistep continuous-flow microsynthesis of magnetic and fluorescent γ-Fe_2O_3@SiO_2 core/shell nanoparticles. Angew. Chem. **121**, 7316–7319 (2009)
24. Descalzo, A.B., Marcos, M.D., Martinez-Manez, R., Soto, J., Bentran, D., Amoros, P.: Anthrylmethylamine functionalised mesoporous silica-based materials as hybrid fluorescent chemosensors for ATP. J. Mater. Chem. **15**, 2721–2731 (2005)
25. Descalzo, A.B., Jimenez, D., El Haskouri, J., Beltran, D., Amoros, P., Marcos, M.D., Martinez-Manez, R., Soto, J.: A new method for fluoride determination by using fluorophores and dyes anchored onto MCM-41. Chem. Commun. **6**, 562–563 (2002)
26. Brasola, E., Mancin, F., Rampazzo, E., Tecilla, P., Tonellato, U.: A fluorescence nanosensor for Cu^{2+} on silica particles. Chem. Commun. **24**, 3026–3027 (2003)
27. Pal, P., Rastogi, S.K., Gibson, C.M., Aston, D.E., Branen, A.L., Bitterwolf, T.E.: Fluorescence sensing of zinc(II) using ordered mesoporous silica material (MCM-41) functionalized with *N*-(quinolin-8-yl)-2-[3-(triethoxysilyl)propylamino]acetamide. ACS Appl. Mater. Interfaces **3**, 279–286 (2011)
28. Han, W.S., Lee, H.Y., Jung, S.H., Lee, S.J., Jung, J.H.: Silica-based chromogenic and fluorogenic hybrid chemosensor materials. Chem. Soc. Rev. **38**, 1904–1915 (2009)
29. Zhang, J.F., Park, M., Ren, W.X., Kim, Y., Kim, S.J., Jung, J.H., Kim, J.S.: A pellet-type optical nanomaterial of silica-based naphthalimide–DPA–Cu(II) complexes: recyclable fluorescence detection of pyrophosphate. Chem. Commun. **47**, 3568–3570 (2011)
30. Xu, X.-D., Wang, X.-G., Lin, B–.B., Cheng, H., Zhang, X.-Z., Zhuo, R.-X.: Interface self-assembly to construct vertical peptide nanorods on quartz template. Chem. Commun. **47**, 7113–7115 (2011)
31. Aragay, G., Pons, J., Merkoci, A.: Recent trends in macro-, micro-, and nanomaterial-based tools and strategies for heavy-metal detection. Chem. Rev. **111**, 3433–3458 (2011)
32. Misra, A., Shahid, M.: Immobilization of self-quenched DNA hairpin probe with a heterobifunctional reagent on a glass surface for sensitive detection of oligonucleotides. Bioorg. Med. Chem. **17**, 5826–5833 (2009)
33. Chen, Y., Droumaguet, C.L., Li, K., Cotham, W.E., Lee, N., Walla, M., Wang, Q.: A novel rearrangement of fluorescent human thymidylate synthase inhibitor analogues in ESI tandem mass spectrometry. J. Am. Soc. Mass Spectrom. **21**, 403–410 (2010)
34. Shahid, M., Srivastava, P., Misra, A.: An efficient naphthalimide based fluorescent dyad (ANPI) for F^- and Hg^{2+} mimicking OR, XNOR and INHIBIT logic functions. New J. Chem. **35**, 1690–1700 (2011)
35. Benesi, H.A., Hildebrand, J.H.: A spectrophotometric investigation of the interaction of iodine with aromatic hydrocarbons. J. Am. Chem. Soc. **71**, 2703–2707 (1949)
36. Joshi, B.P., Lohani, C.R., Lee, K.H.: A highly sensitive and selective detection of Hg(II) in 100 % aqueous solution with fluorescent labeled dimerized Cys residues. Org. Biomol. Chem. **8**, 3220–3226 (2010)
37. McQuade, L.E., Lippard, S.J.: Fluorescence-based nitric oxide sensing by Cu(II) complexes that can be trapped in living cells. Inorg. Chem. **49**, 9535–9545 (2010)
38. Misra, A., Shahid, M.: Chromo and fluorogenic properties of some azo-phenol derivatives and recognition of Hg^{2+} ion in aqueous medium by enhanced fluorescence. J. Phys. Chem. C **114**, 16726–16739 (2010)